Structural Optimization 12, 98–105 © Springer-Verlag 1996

Stress-based topology optimization

R.J. Yang and C.J. Chen

Ford Motor Company, P.O. Box 2053, MD 2122-SRL, Dearborn, MI 48121, USA

Abstract Previous research on topology optimization focussed primarily on global structural behaviour such as stiffness and frequencies. However, to obtain a true optimum design of a vehicle structure, stresses must be considered. The major difficulties in stress based topology optimization problems are two-fold. First, a large number of constraints must be considered, since unlike stiffness, stress is a local quantity. This problem increases the computational complexity of both the optimization and sensitivity analysis associated with the conventional topology optimization problem. The other difficulty is that since stress is highly nonlinear with respect to design variables, the move limit is essential for convergence in the optimization process. In this research, global stress functions are used to approximate local stresses. The density method is employed for solving the topology optimization problems. Three numerical examples are used for this investigation. The results show that a minimum stress design can be achieved and that a maximum stiffness design is not necessarily equivalent to a minimum stress design.

1 Introduction

Topology optimization has been extensively studied with stiffness and frequency considerations in the literature (Park 1995; Bendsøe and Kikuchi 1988; Ma *et al.* 1995; Díaz and Kikuchi 1992; Rozvany *et al.* 1992; Jog *et al.* 1994; Mlejnek and Schirrmacher 1993; Yang and Chahande 1995; Yang and Chuang 1994; Gea 1994; Wang *et al.* 1996). It was demonstrated that a light weight and high stiffness design can be achievable. However, a high stiffness design may result in low durability, if stress is not considered in the design process.

There has been relatively little research done on stress based topology optimization problems and among them only truss elements which are seldom used in the automotive industry have been investigated (Cheng and Jiang 1992; Sankaranaryanan *et al.* 1992). Rozvany *et al.* (1995) proposed a new optimality criteria method DCOC to perform stress based topology optimization. Harzheim *et al.* (Baumgartner *et al.* 1992; Harzheim and Graf 1995) used a biological growth concept and an optimality criteria method to determine the optimal topology for the reduction of structural peak stress. The Young's moduli were varied as functions of stress to obtain the fully stressed design. The drawback of this method is its lack of generality. It is unable to handle other design criteria such as stiffness and frequency.

Stress based topology optimization problems are faced with two major difficulties: stress is a local quantity and stress is highly nonlinear with respect to the design variables. Because of its high nonlinearity, the move limit needs to be considered with special care to ensure convergence. Unlike stiffness, since stress is a local quantity, a large number of constraints must be considered. By increasing the complexity of both the optimization algorithm and sensitivity analysis, these problems add to the computational time associated with the topology optimization, which already considers a large number of design variables. This research considers stress reduction in the topology optimization process. The local stresses are first transformed to a global stress function which is then used in the optimization process. Two global stress functions are investigated: the Kreisselmeier-Steinhauser function (KS) and the function proposed by Park and Kikuchi (KK) (Park 1995). The density method or the engineering method is used to perform the topology optimization (Mlejnek and Schirrmacher 1993; Yang and Chahande 1995; Yang and Chuang 1994) and MSC/NASTRAN is used to conduct the finite element analysis. The continuum adjoint variable method is employed for efficient sensitivity analysis (Yang and Chuang 1994; Haug *et al.* 1986) which is briefly discussed in the following section. Three optimization problems are formulated, optimized, and discussed.

2 Optimization formulations

One of the solutions for solving the local stress problem is to transform the stresses to a global stress measure. The global stress measure is then treated as the only constraint in the optimization process. The advantages are obvious. It reduces the burden for the optimization algorithm and solves a topology optimization problem similar to that in the literature. It also reduces the computational cost for calculating the elemental stress sensitivities which are quite intensive considering the numbers of design variables and constraints. The disadvantage is that it is difficult to find a general and robust function that can be applied to all cases for stress reduction.

Two global stress functions are investigated: the Kreisselmeier-Steinhauser (KS) and the function proposed by Park and Kikuchi (KK) (Park 1995). The KS function is in the form of

$$G_{\mathrm{ks}} = \frac{1}{p} \ln \sum_{i=1}^{N} e^{p \frac{f_i(\sigma)}{f_{\max}(\sigma)}}, \tag{1}$$

where N is the number of finite elements in the design domain, σ is the stress, $f_{\max}(\sigma)$ is the maximum von Mises stress, and $f_i(\sigma)$ is the von Mises stress for each finite element. The parameter p determines the difference between the original function and its approximation. When a high value of p is used, the peak stress is weighted more heavily. However, it often leads to oscillation or even divergence during the optimization iterations. The oscillation results from the high nonlinearity of the global stress function. Here, $p = 20$

is chosen, as selecting the optimal p is beyond the scope of this research.

The mathematical form of the KK function, which is the p-norm of local stresses, is written as (Park 1995)

$$G_{\mathrm{kk}} = \left\{ \int_{\Omega} \left[\frac{f_i(\sigma)}{f_{\max}(\sigma)} \right]^p \mathrm{d}\Omega \right\}^{\frac{1}{p}}, \tag{2}$$

where Ω is the design domain, and $p = 20$ as before.

One compliance minimization and two stress optimization problems are formulated and discussed as follows.

2.1 Compliance minimization problem (CM)

The compliance topology optimization problem is the most common in the literature. It is solely used for benchmarking. The optimization formulation is

$$\begin{aligned} &\min \quad C, \\ &\text{subject to} \quad \int_{\Omega} \rho \,\mathrm{d}\Omega \leq M_0, \end{aligned} \tag{3}$$

where C is the compliance, Ω is the design domain, ρ is the material density, and M_0 is the total material usage. Note that the compliance minimization problem is equivalent to the stiffness maximization problem and that stresses are not considered in this case.

2.2 Stress minimization problem (SM)

Instead of compliance, stress is chosen as the objective function. The optimization problem is as follows:

$$\begin{aligned} &\min \quad G, \\ &\text{subject to} \quad \int_{\Omega} \rho \,\mathrm{d}\Omega \leq M_0, \end{aligned} \tag{4}$$

where G is the global stress function of von Mises stress.

2.3 Compliance and stress minimization problem (CSM)

To consider structural stiffness and stress, a linear, weighted function is employed as the objective function

$$\begin{aligned} &\min \quad c_1 C + c_2 G, \\ &\text{subject to} \quad \int_{\Omega} \rho \,\mathrm{d}\Omega \leq M_0, \end{aligned} \tag{5}$$

where c_1 and c_2 are the weighting factors for the compliance and the global stress function, respectively. Since stress minimization is a major concern, a larger weighting factor is assigned to global stress function, i.e. $c_1 = 0.3, c_2 = 0.7$. It is noted that many combinations of c_1 and c_2 can be selected, however, it is beyond the scope of this research.

3 Design sensitivity analysis

Sensitivity analysis plays a major role in the topology optimization process. Efficient and accurate sensitivity can achieve fast convergent results, which translates to major cost savings. Since only one stress function is treated, the continuum adjoint variable method is used to achieve computational efficiency (Yang and Chuang 1994; Haug *et al.* 1986). The design variable for the density method is the normalized material density of each finite element. In the following, the design sensitivity of the global stress function with respect to the normalized density ρ is derived.

The variational form of the elasticity problem is written as

$$a_\rho(\mathbf{z}, \overline{\mathbf{z}}) = \ell_\rho(\overline{\mathbf{z}}), \quad \text{for all } \overline{\mathbf{z}} \in \mathbf{Z}, \tag{7}$$

where

$$a_\rho(\mathbf{z}, \overline{\mathbf{z}}) = \int_{\Omega} \sigma^{ij}(\mathbf{z}) \varepsilon^{ij}(\overline{\mathbf{z}}) \,\mathrm{d}\Omega, \tag{8}$$

and

$$\ell_\rho(\overline{\mathbf{z}}) = \int_{\Omega} \mathbf{F}^T \overline{\mathbf{z}} \,\mathrm{d}\Omega. \tag{9}$$

In (7)-(9), $\mathbf{z}$ and $\overline{\mathbf{z}}$ are the real and virtual displacement vectors, $\mathbf{Z}$ is the space of kinematically admissible displacements, $\rho \in \mathbf{R}$ is the normalized material density, σ^{ij} and ε^{ij} are stress and strain tensor, respectively, and $\mathbf{F}$ is the external loading. The first-order variation of (7) with respect to the density variables is written as (Haug *et al.* 1986)

$$a_\rho(\mathbf{z}', \overline{\mathbf{z}}) = \ell'_{\delta\rho}(\overline{\mathbf{z}}) - a'_{\delta\rho}(\mathbf{z}, \overline{\mathbf{z}}), \tag{10}$$

where

$$a_\rho(\mathbf{z}', \overline{\mathbf{z}}) = \int_{\Omega} \sigma^{ij}(\mathbf{z}') \varepsilon^{ij}(\overline{\mathbf{z}}) \,\mathrm{d}\Omega, \tag{11}$$

$$\ell'_{\delta\rho}(\overline{\mathbf{z}}) = \int_{\Omega} \mathbf{F}'^T \overline{\mathbf{z}} \,\mathrm{d}\Omega, \tag{12}$$

and

$$a'_{\delta\rho}(\mathbf{z}, \overline{\mathbf{z}}) = \int_{\Omega} \varepsilon^{ij}(\mathbf{z}) \left(\mathbf{D}^{ijk\ell} \right)' \varepsilon^{k\ell}(\overline{\mathbf{z}}) \,\mathrm{d}\Omega, \tag{13}$$

where $\mathbf{D}^{ijk\ell}$ is the elasticity tensor and $(D^{ijk\ell})'$ is its derivative.

The first-order variation of the stress functional $G = \int g(\rho, \mathbf{z}) \,\mathrm{d}\Omega$ is

$$G' = \int g' + g_{\mathbf{z}} \mathbf{z}' \,\mathrm{d}\Omega. \tag{14}$$

Based on (14), the adjoint equation for the stress functional is defined as

$$a_\rho(\lambda, \overline{\lambda}) = \int g_{\mathbf{z}} \overline{\lambda} \,\mathrm{d}\Omega, \quad \text{for all } \overline{\lambda} \in \mathbf{Z}, \tag{15}$$

where $\overline{\lambda}$ is the virtual displacement and $\mathbf{Z}$ is the space of kinematically admissible displacements.

By setting $\overline{\lambda} = \mathbf{z}' \in \mathbf{Z}$ in (15) and $\overline{\mathbf{z}} = \lambda \in \mathbf{Z}$ in (10) and then using the symmetry property of the energy bilinear form $a_\rho(*,*)$, the design sensitivity of the stress function with respect to design variables is written as

$$G' = \ell'_{\delta\rho}(\lambda) - a'_{\delta\rho}(\mathbf{z}, \lambda) + \int g' \,\mathrm{d}\Omega. \tag{16}$$

Unlike the compliance sensitivity (Yang and Chuang 1994; Haug *et al.* 1986), (16) shows that one additional finite element analysis (FEA) is required for obtaining the stress sensitivity.

4 Numerical examples and discussion

Three numerical examples were used to investigate the effects of the move limit, global stress function, and different optimization formulations. The termination criterion for optimization is the maximum iteration number which is chosen as 10 for all cases. The detailed finite element and other design information are given in the following.

4.1 P1: clamped solid beam

The first example is a clamped solid beam with concentrated loads applied at the centre, as shown in Fig. 1. The finite element model includes 1107 grid points and 640 8-node HEX elements. The material usage for this example is limited to 50%.

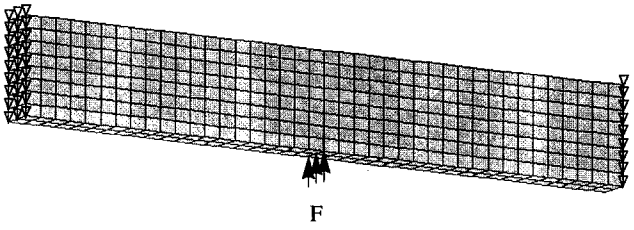

Fig. 1. Clamped solid beam

4.2 P2: clamped shell beam

The second example is a clamped shell beam with loading applied at the centre of the top surface, as shown in Fig. 2. The finite element model includes 1377 grid points, 1280 CQUAD4 elements, and more than 6700 degrees of freedom. The material usage for this example is limited to 70%.

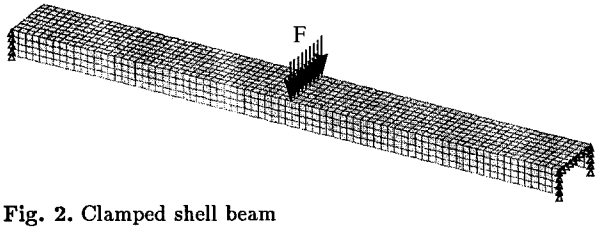

Fig. 2. Clamped shell beam

4.3 P3: simplified vehicle body structure

The third example is a simplified vehicle body structure with torsional loads, as shown in Fig. 3. The finite element model includes 5456 QUAD4 and 20 TRIA3 elements, 5508 grid points, and more than 33,000 degrees of freedom. The design is to minimize stress and compliance with 25% material usage constraint imposed on the floor panel, i.e., the floor panel is the design domain.

4.4 Move limit

The move limit is the parameter to determine how far the current design can go in one design iteration. For a compliance minimization problem, the move limit can be very large, e.g. 50%. Unfortunately, it cannot be applied to the stress problem because of its high nonlinearity. Two move limits: 10% and 20% are used in this study.

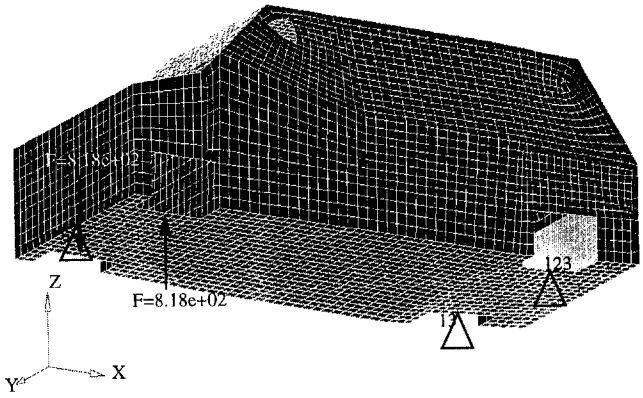

Fig. 3. Simplified body structure

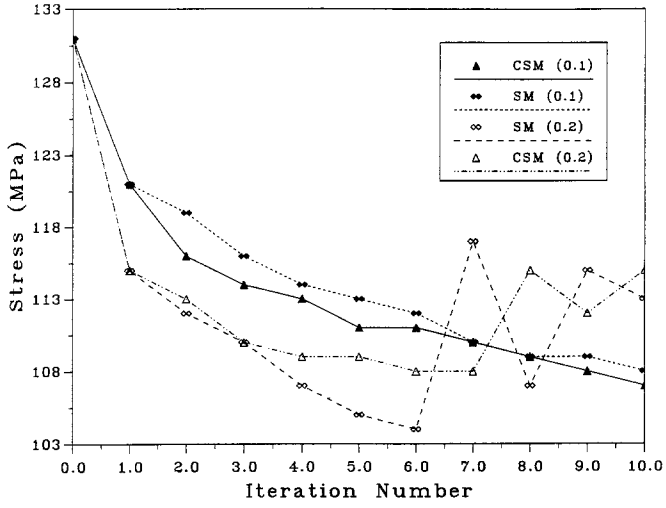

Fig. 4(a) Solid beam stress

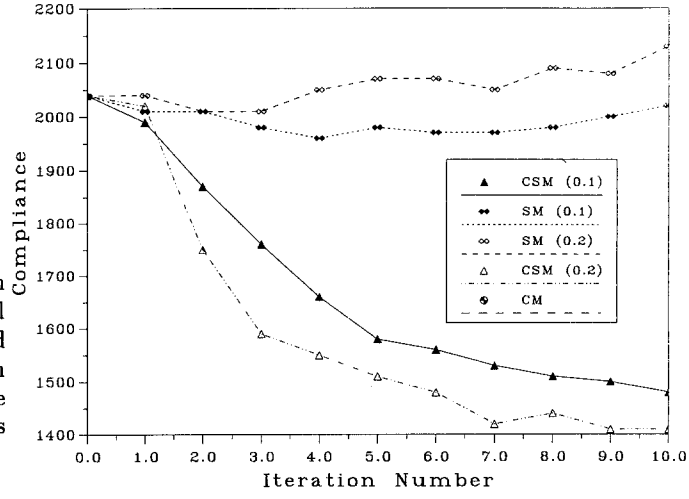

Fig. 4(b) Solid beam compliance

Figures 4a to d show the design histories for the peak stress and the compliance. Figures 4a and b are for the solid beam example ($P1$) and Figs. 4c and d are for the shell beam example ($P2$). It is observed that, in general, the variations in stresses are larger than those in compliances and that the

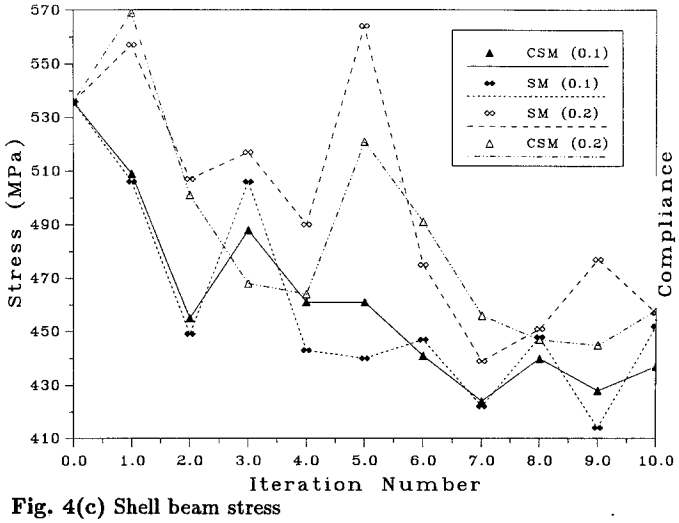

Fig. 4(c) Shell beam stress

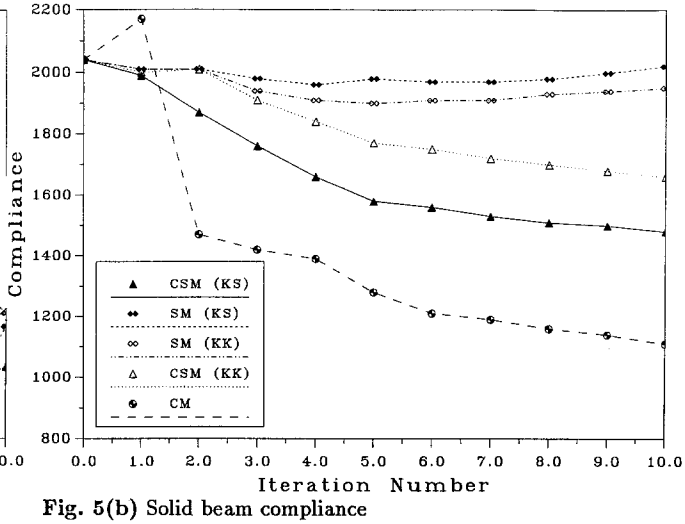

Fig. 5(b) Solid beam compliance

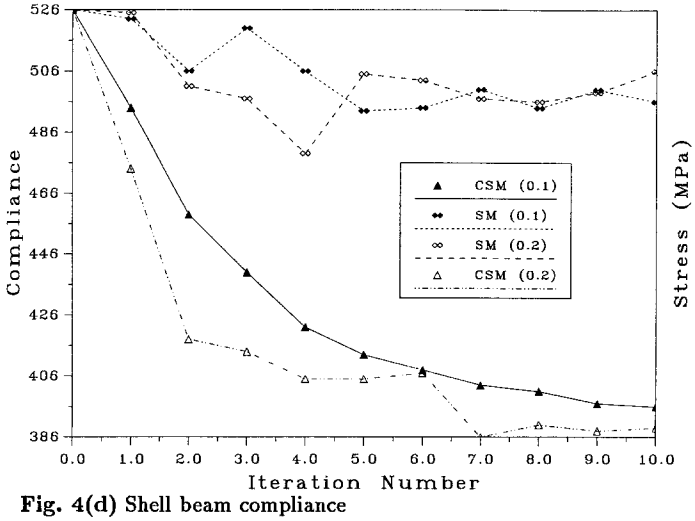

Fig. 4(d) Shell beam compliance

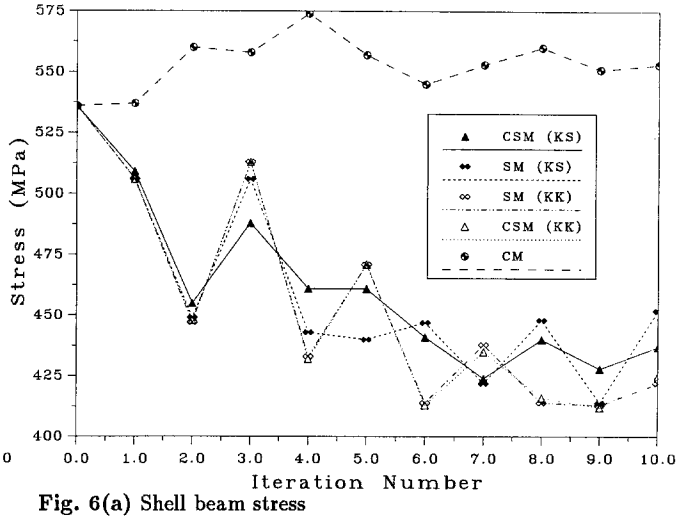

Fig. 6(a) Shell beam stress

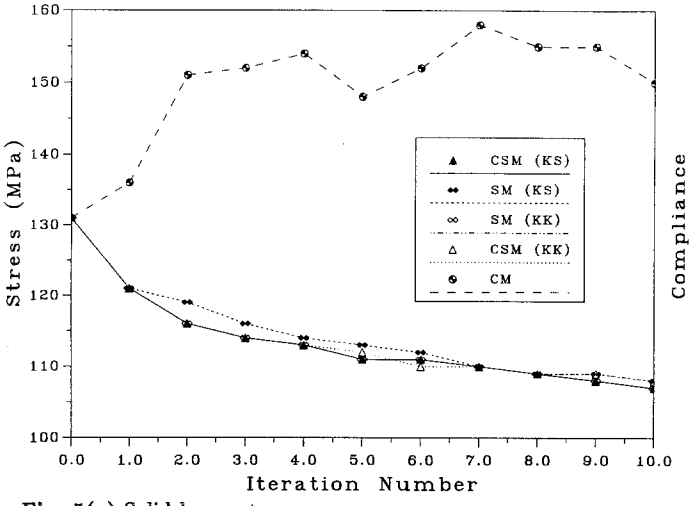

Fig. 5(a) Solid beam stress

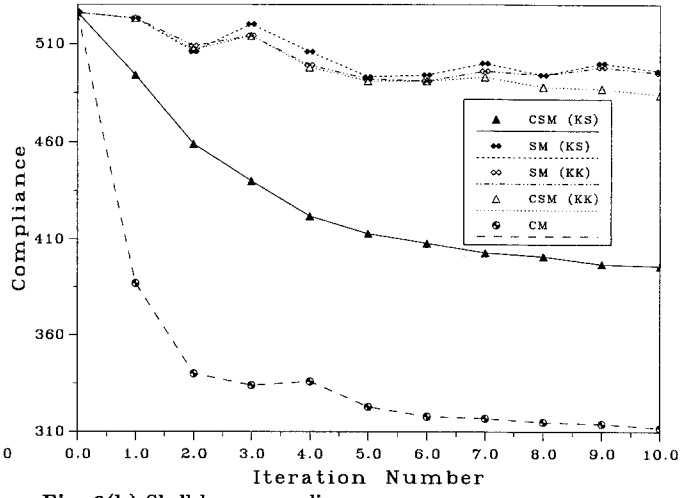

Fig. 6(b) Shell beam compliance

10% move limit is more stable than the 20% move limit. The stress variations may depend on the choice of parameter p for the global stress function. A large parameter p or a large move limit may result in a divergent solution. Comparing

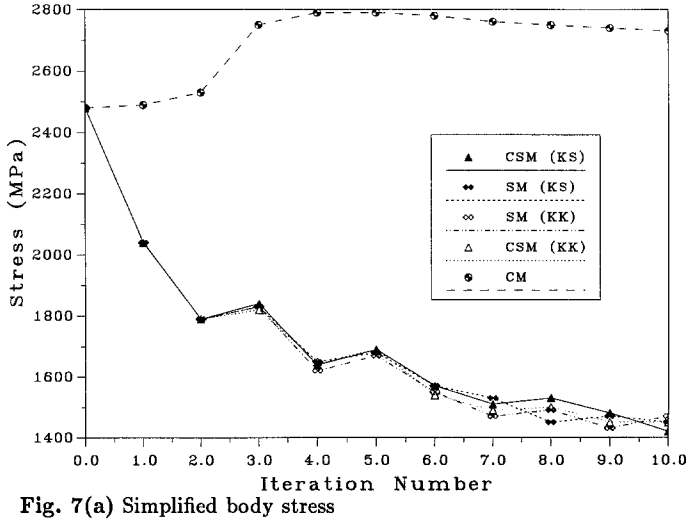

Fig. 7(a) Simplified body stress

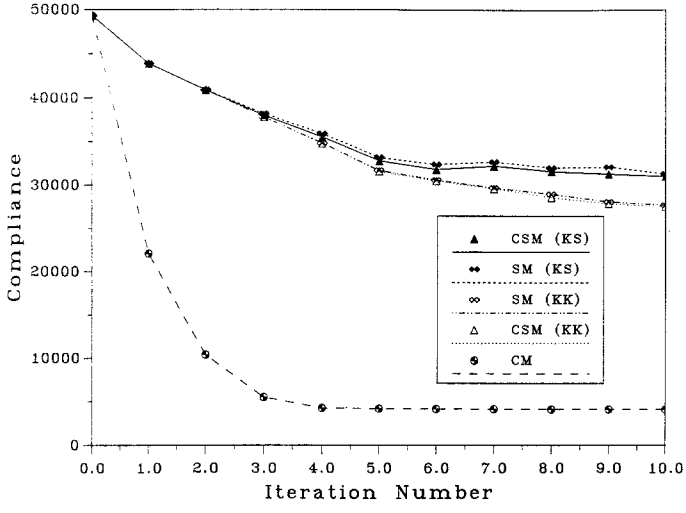

Fig. 7(b) Simplified body compliance

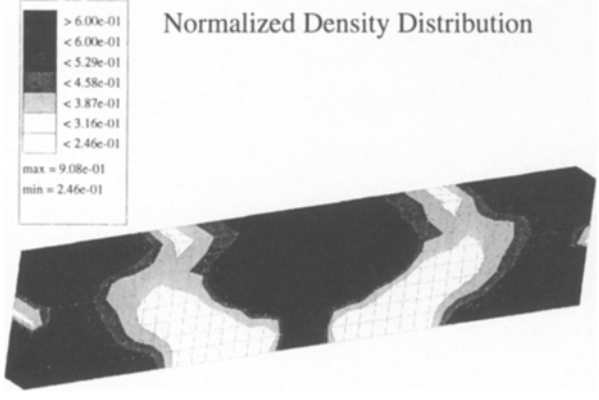

Fig. 8(a) Material distribution for $P1$ (SM, KS)

the CSM and SM with fixed move limit, the CSM formulation is more stable than the SM. This may result from the contribution of a smoother compliance function to the objective function of CSM. It is also found that more drastic stress jumps occur during the design iterations for the shell element

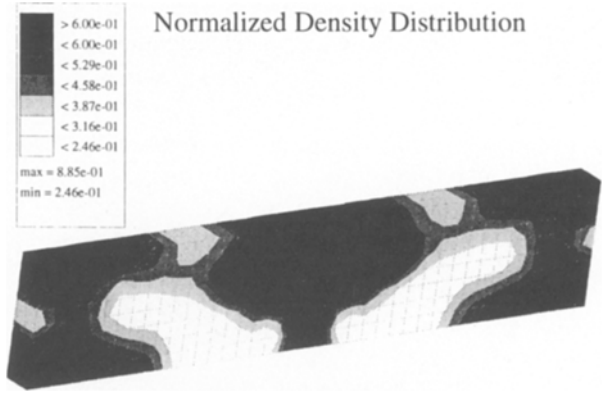

Fig. 8(b) Material distribution for $P1$ (SM, KK)

model than for the solid element model. In the following, a 10% move limit is employed unless otherwise specified.

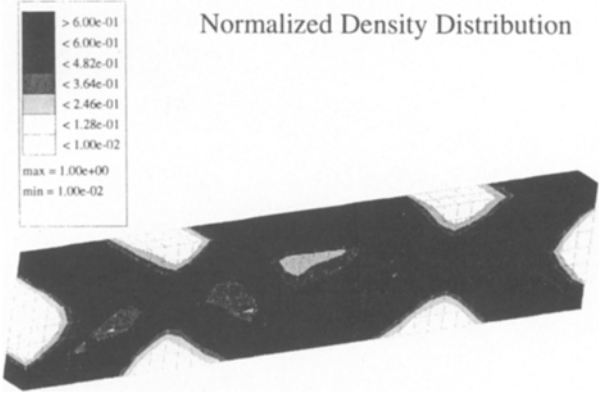

Fig. 8(c) Material distribution for $P1$ (CM)

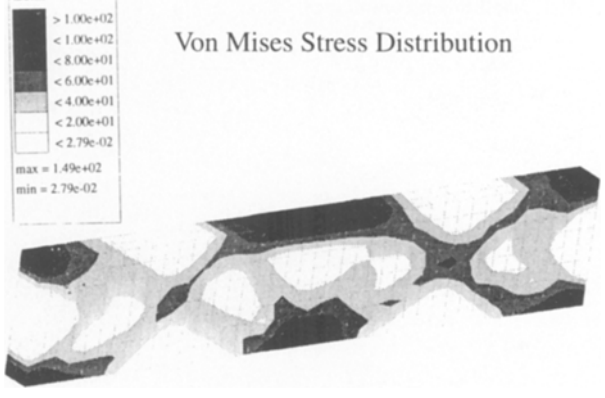

4.5 Global stress function

Two global stress functions were studied. The KS function in (1) and the KK function in (2) were applied and compared. The results are shown in Figs. 5 to 7 for $P1$, $P2$, and $P3$, respectively. It is noted that both global stress functions produce comparable results. The stresses for all three problems

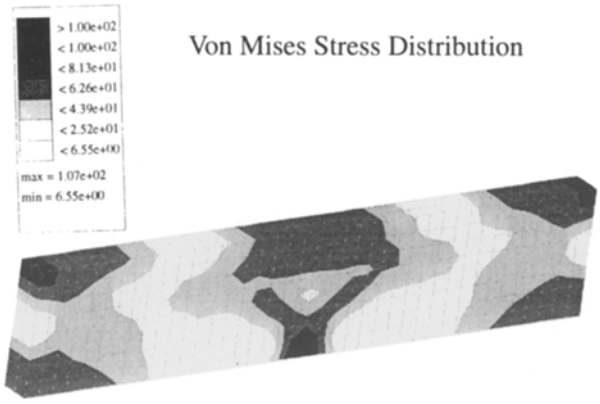

Fig. 8(e) Stress distribution for $P1$ (SM, KS)

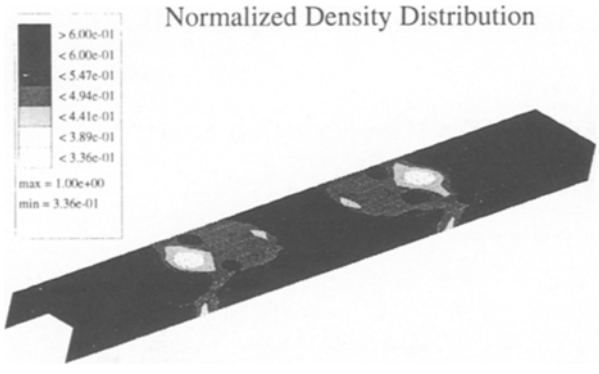

Fig. 9(a) Material distribution for $P2$ (SM, KS)

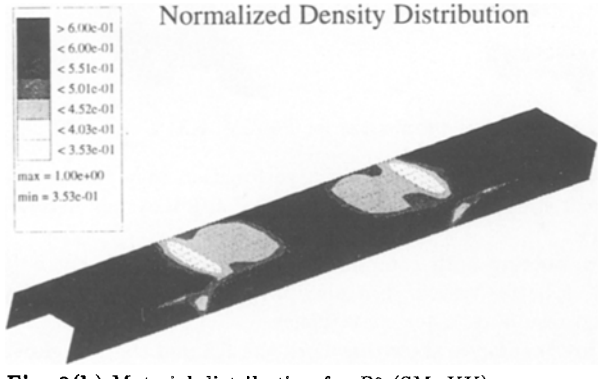

Fig. 9(b) Material distribution for $P2$ (SM, KK)

were reduced and convergent results were reached. The peak stresses for $P1$ and $P2$ are reduced by more than 15% and for $P3$ the peak stress is reduced by more than 40%.

The material distribution results of the SM formulation for all examples are shown in Figs. 8 to 10. Similar topology contours were obtained for both KS and KK stress functions. Figures 8a and b show the optimal material distributions of $P1$, using the KS and KK global stress functions, respectively. Figures 9a and b and Figs. 10a and b are the optimal material distributions for $P2$ and $P3$, respectively.

4.6 Optimization problems

Three optimization formulations were implemented: CM, CSM, and SM. The design histories for all examples are

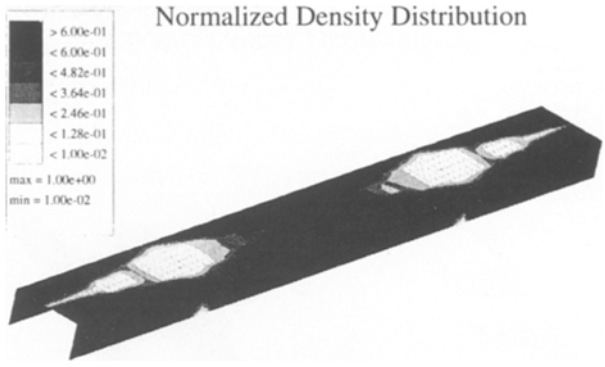

Fig. 9(c) Material distribution for $P2$ (CM)

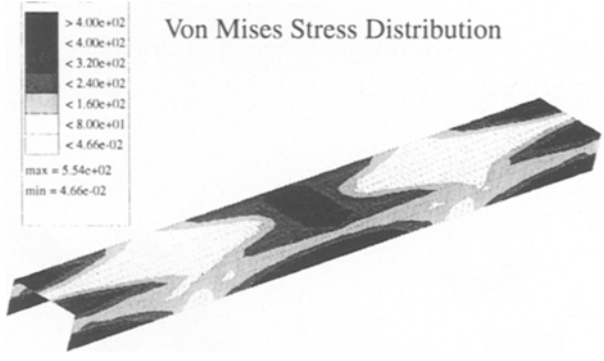

Fig. 9(d) Stress distribution for $P2$ (CM)

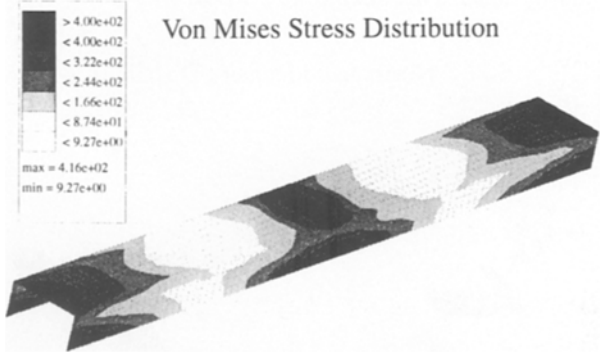

Fig. 9(e) Stress distribution for $P2$ (SM, KS)

shown in Figs. 5 to 7. In general, the results show that the stress increases if the compliance is the objective function (CM) and the compliance increases if the stress is the objective function (SM). The CSM formulation shows that it can improve both stiffness and stresses.

It is noted that the final topologies for SM and CM are quite different. This indicates that the maximum stiffness design is not equivalent to the minimum stress design. Figures 8a and c, Figs. 9a and c, Figs. 10a and c show the optimal material distributions of SM and CM for $P1$, $P2$, and $P3$, respectively.

It is also noted that the patterns for final material and stress distribution are similar for both CM and SM. Figures 8a and e, Figs. 9a and e, and Figs. 10a and e show the optimal material and stress distributions of SM for $P1$, $P2$, and $P3$. Figures 8c and d, Figs. 9c and d, and Figs. 10c and d show the

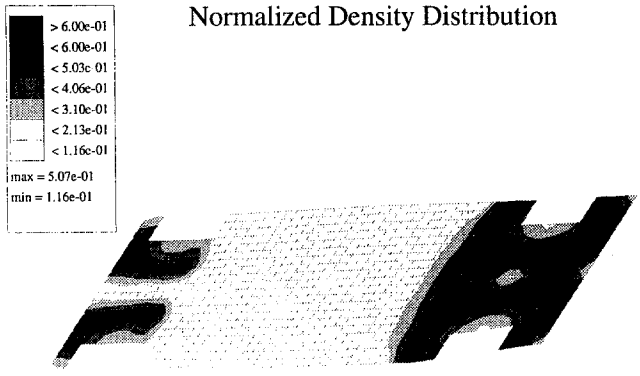

Fig. 10(a) Material distribution for $P3$ (SM, KS)

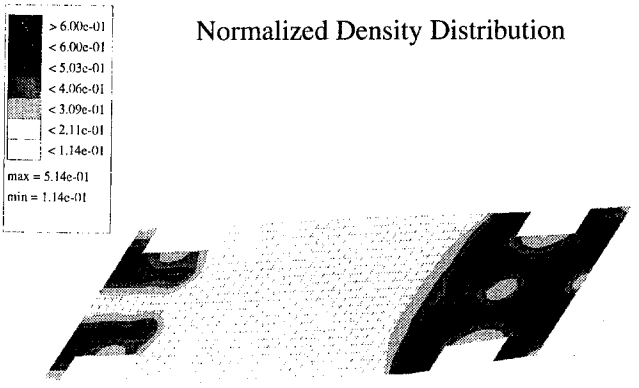

Fig. 10(b) Material distribution for $P3$ (SM, KK)

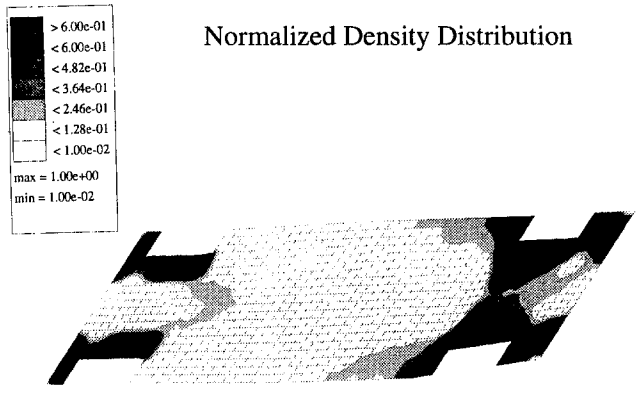

Fig. 10(c) Material distribution for $P3$ (CM)

optimal material and stress distributions of CM for $P1$, $P2$, and $P3$, respectively. The CSM results are between those of SM and CM as expected and thus are omitted.

5 Conclusions

The stress based topology optimization problem has been investigated. Based on the numerical investigation, the following observations and conclusions are drawn.

- Reduction of both the peak stress and the structural compliance is achievable.
- The maximum stiffness design is not equivalent to the minimum stress design.

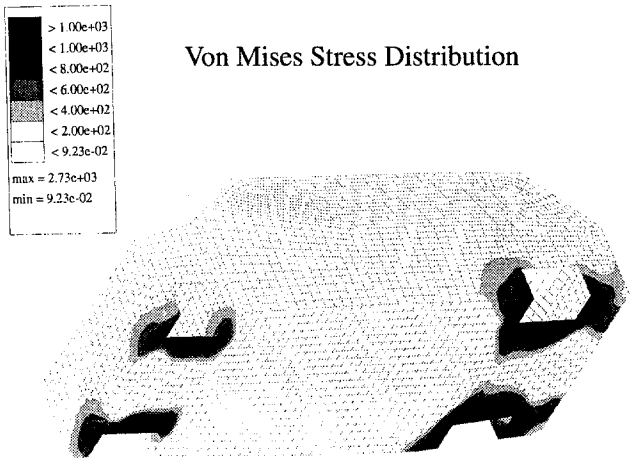

Fig. 10(d) Stress distribution for $P3$ (CM)

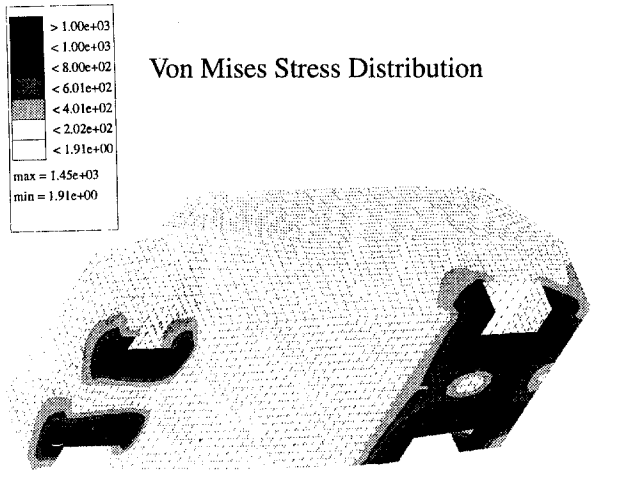

Fig. 10(e) Stress distribution for $P3$ (SM, KS)

- Treating stress as the objective function may reduce the peak stress, however, the structural stiffness may deteriorate.
- Considering both compliance and stress (CSM), not only gives better results, but also provides numerical stability and results in faster convergence.
- Three examples show that both the KS and the KK global stress function are comparable and can achieve stress reduction.
- Numerical results show that final topology contours are similar to final stress contours.
- The global stress function is highly nonlinear and is sensitive to the optimization move limit. To ensure convergence, 10% move limit was used in this study.

Acknowledgement

The authors wish to express appreciation to M. Chiredast for providing the body structure model.

References

Baumgartner, A.; Harzheim, L.; Mattheck, C. 1992: SKO: the biological way to find an optimum structure topology. *Int. J.*

Fatigue **14**, 387-393

Bendsøe, M.P.; Kikuchi, N. 1988: Generating optimal topologies in structural design using a homogenization method. *Comp. Meth. Appl. Mech. Eng.* **71**, 197-224

Cheng, G.; Jiang, Z. 1992: Study on topology optimization with stress constraints. *Eng. Opt.* **20**, 129-148

Díaz, A.; Kikuchi, N. 1992: Solution to shape and topology eigenvalue optimization problem using a homogenization method. *Int. J. Num. Meth. Eng.* **35**, 1487-1502

Gea, H.C. 1994: Topology optimization: a new micro-structure based design domain method. *ASME Advances in Design Automation* **2**, 283-290

Harzheim, L.; Graf, G. 1995: Optimization of engineering components with the SKO method. *SAE Vehicle Struct. Mech. Conf.* (held in Troy, MI), pp. 235-243

Haug, E.J.; Choi, K.K.; Komkov, V. 1986: *Design sensitivity analysis of structural systems.* New York: Academic Press

Jog, C.S.; Haber, R.B.; Bendsøe, M.P. 1994: Topology design with optimized, self-adaptive materials. *Int. J. Num. Meth. Eng.* **37**, 1323-1350

Ma, Z.D.; Kikuchi, N.; Cheng, H.C.; Hagiwara, I. 1995: Topological optimization technique for free vibration problems. *Trans. ASME, J. Appl. Mech.* **62**, 200-207

Mlejnek, H.P.; Schirrmacher, R. 1993: An engineer's approach to optimal material distribution and shape finding. *Comp. Meth. Appl. Mech. Eng.* **106**, 1-26

Park, Y.K. 1995: *Extensions of optimal layout design using the homogenization method.* Ph.D. Thesis, University of Michigan, Ann Arbor

Rozvany, G.I.N.; Bendsøe, M.P.; Kirsch, U. 1995: Layout optimization of structures. *Appl. Mech. Rev.* **48**, 41-117

Rozvany, G.I.N.; Zhou, M.; Birker, T. 1992: Generalized shape optimization without homogenization. *Struct. Optim.* **4**, 250-252

Sankaranaryanan, S.; Haftka, R.T.; Kapania, R.K. 1992: Truss topology optimization with stress and displacement constraints. In: Bendsøe, M.P.; Mota Soares, C.A. (eds.) *Topology design of structures*, pp. 71-78. Dordrecht: Kluwer

Wang, B.P.; Lu, C.M.; Yang, R.J. 1996: Optimal topology for maximum eigenvalue using density-dependent material model. *37th AIAA/ASME/ASCE/AHS/ASC Structures, Struct. Dyn. Mat. Conf.* (held in Salt Lake City, UT), pp. 2644-2652

Yang, R.J.; Chahande, A.I. 1995: Automotive applications of topology optimization. *Struct. Optim.* **9**, 245-249

Yang, R.J.; Chuang, C.H. 1994: Optimal topology design using linear programming. *Comp. & Struct.* **52**, 265-275

Received Nov. 13, 1995
Revised manuscript received Jan. 21, 1996